Renewable Energy 147 (2020) 1500–1510

Contents lists available at ScienceDirect

Renewable Energy

journal homepage: www.elsevier.com/locate/renene

# Experimental investigation on varying flame characteristics of benzoic resin solid fuel pellets

Ravikumar Sankaralingam [a, c], Balasubramanian Sengottuvelan [b], Pranesh Venkat [c, *], Mahalingam Selvaraj [d], Velmurugan Arunachalam [e, f], Jeyakumaran Natarajan [g]

[a] Department of Mechanical Engineering, Jeppiaar Maamallan Engineering College, Sriperumbudur, Tamil Nadu, 602108, India
[b] Department of Inorganic Chemistry, University of Madras, Chennai, Tamil Nadu, 600025, India
[c] Minerals and Chemicals Division, Dawn Calorific Exports, Chennai, Tamil Nadu, 600033, India
[d] Department of Mechanical Engineering, Sona College of Technology, Salem, Tamil Nadu, 636005, India
[e] Department of Mechanical Engineering, Annamalai University, Chidambaram, Tamil Nadu, 608002, India
[f] Department of Mechanical Engineering, Government College of Engineering, Dharmapuri, Tamil Nadu, 636704, India
[g] Department of Physics, V.H.N. Senthikumara Nadar College, Virudhunagar, Tamil Nadu, 626001, India

ARTICLE INFO

*Article history:*
Received 4 December 2018
Received in revised form
11 September 2019
Accepted 14 September 2019
Available online 18 September 2019

*Keywords:*
Benzoic resin
Gas chromatography
FESEM
Flame characteristics
Mathematical model
Heat release rate

ABSTRACT

This paper discusses about the varying flame characteristics of a solid fuel known as benzoic resin as a function of surface temperature and time. Benzoic resin is a naturally occurring biomass and the solid fuel is synthesized using different species of tree bark from the genus Styrax. Hence, an induction heating steel plate fitted with liquefied petroleum gas (LPG) flame ignitor was employed to evaluate these characteristics. Furthermore, a mathematical model is developed to estimate and predict the changing flame behavior of benzoic resin solid fuel. Experiments were executed for different heating surface temperatures such as 70 °C, 110 °C, 130 °C, 160 °C, 180 °C, 210 °C, 240 °C, and 270 °C. The experimental results revealed that there was a change in the flame behavior at 70 °C and 110 °C surface temperatures. The nature of the flames were transition and turbulent, but the laminar flame was detected only at the induction heating surface temperatures of 160 °C and 270 °C. Also, the laminar flame angle is 90° under uniform surface heat flux. Moreover, increase in heat release rate was observed for increasing combustion time.



## 1. Introduction

Solid biomass has emerged as an essential renewable energy source with enormous production capacity [1] and it has become a vital energy resource for thermal energy production due to its exceptional combustion performance [2]. Besides, coal is a major component in the production of steel and generation of electricity. In contrast, it is a potential contributor to the enhancement of carbon dioxide ($CO_2$) emission intensity and climate change. Carbon dioxide emission makes 70% share in greenhouse gas emissions and this is due to high usage of coal in metallurgical industries [3]. On the other hand, the demand for coal is increasing in the developing economies such as India and China. These countries are leading in the carbon dioxide emissions and coal is an indispensable energy source in their economic development. The rapid consumption, depletion and emissions of coal reserves and their consequent climate change has necessitated to explore a new renewable energy fuel that could be a supplement or replacement for coal. For that purpose, this paper presents benzoic resin solid fuel to the scientific community and this solid fuel is equivalent to coal, based on its chemical properties. But, this work mainly describes the flame characteristics of this solid fuel. Fig. 1 shows the photograph of the benzoic resin solid fuel pellets. Pranesh et al. (2018) [4], have investigated the ignition behavior of benzoic resin solid fuel pellets over a surface induction heating plate using a liquefied petroleum gas flame ignitor. The authors studied the ignition and heat release rate properties of this solid fuel. Additionally, FTIR and microstructural images were investigated. The benzoic resin exhibits a honeycomb structure and rapid ignition and linear heat release were noted for increasing surface temperature and combustion time. Benzoic resin is a naturally occurring biomass and it is a solid biofuel. It is a balsamic resin that has been

* Corresponding author.
*E-mail address:* venkat.pranesh@outlook.com (P. Venkat).

https://doi.org/10.1016/j.renene.2019.09.061
0960-1481/

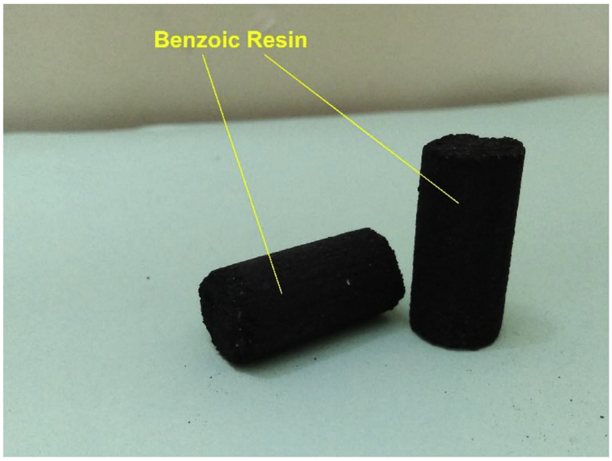


**Fig. 1.** Benzoic Resin Pellets used for the Analysis [4].

synthesized using different species of tree bark from the genus Styrax. A huge amount of this biomass energy resource is available in nature, and it is very difficult to provide the accurate quantity. Actually, this is a processed fuel, which is obtained from the barks of various balsam trees that are native to tropical countries. The chemical properties of benzoic resin have been investigated. [5,6], and [7]. Certainly, this product is a potential supplement to a solid and pulverized coal. Kashio and Johnson (2001) [8], reviewed and the history, chemistry, production, and economics of the balsamic resin from styrax species. They pointed out that there are several forms of benzoin in the international trade and mainly, enormous production and exports of benzoin resin is from Malaysia., Benzoin is the chief constitute for benzoic acid. And it is actually an aromatic carboxylic acid derived from the gum benzoin.

Hovaneissian et al. (2008) [9], conducted analytical investigation on styrax and benzoin balsams by high performance liquid chromatography with photodiode array detector (HPLC-PAD-fluorimetry) and gas chromatography-mass spectrometry (GC-MS). The authors performed the study on the oleoresins styrax and benzoin produced by various East-Asian, American, Mediterranean trees. They also mentioned that this product extensively employed in ancient times for its therapeutic and odoriferous properties.

Fernandez et al. (2006) [10], examined the benzoin gums volatile constituents. The authors used electronic nose device to detect the aromatic (odor) components and chemical makeup of 56 benzoin gum samples of Siam and Sumatra origins. The device detection results reveal that the samples are of different quality grades and this helps them to choose or allocate the best raw material (benzoic gum) for manufacturing of cosmetic, perfume, food, and tobacco products.

Basically, benzoic resin is an incense and widely used for ritual purposes in Asia. Already, Pranesh et al. (2018) [4], have demonstrated that this solid mass benzoic resin is a fuel, which has a gross calorific content of 26,004.92 kJ/kg, and for many decades, it has been viewed in a wrong way and due to lack of out of the box thinking and approach the fuel nature of this benzoic resin is not recognized. Definitely, this product is considered as a supplement solid fuel to coal.

Generally, the knowledge about the ignition, combustion, and flame behaviors of various coals (solid fuels) is absolutely essential in the design of furnace and other thermal engineering systems. As this guide in the determination of temperature gradients on that system and also, this paper tries to the fill the literature gap of the benzoic resin solid fuel's flame behavior as a function of surface temperature. In fact, Katzer et al. [11], analyzed the qualitative and quantitative relationship between pulverized coal flame length and swirl burner at different operating conditions. The authors developed a novel methodology for flame length estimation and presented two algorithms to acquire the video images of coal flame jet and allow the characterization of flame length and its fluctuation as well. The variation in thermal loads of coal burner, secondary air streams, and change in the angle of swirler constructional assemblies, resulted in discrete alterations in the pulverized coal jet flame length. Overall, the authors bridged the research gap of design and operational parameters of the swirl burner with premixed diffusing chamber effects on changing coal jet flame. Additionally, Smart et al. [12], characterized the oxy-coal flame using digital imaging and image processing techniques. The authors initially evaluated the flame behavior by vision-based flame monitoring system and conducted experiments on a coal combustion facility of 0.5 $MW_{th}$ with different oxygen levels in furnace and flue gas recycle ratio. Their results revealed that the temperature of flame decreases with recycle ratio for both test coals indicating that the flame temperature is absolutely dominated by the recycle ratio of flue gas. Also, high content of carbon dioxide in flue gas decrease the flame temperature and, thereby, affecting the flame stability.

Also, Bai et al. [13], numerically investigated the two-phase flame structures in a simplified coal jet flame. The coal particle distributions and general flame features were investigated and furthermore, different coal jet flames namely stripe, s

continuous, and interspersed flames were identified. The three flames exhibit similar gaseous reaction and also, there is a governance of non-premixed flame. The strong reaction is expected to appear in the zones with high rate of scalar dissipation and small vorticity. Additionally, it was revealed that the rate of heat release is less for interspersed flame and 26% was contributed by stripe flame, and this is an important parameter in the determination of stable flame formation. These reports indicate the significance of coal flames for various applications, especially in the design of thermal systems and understanding the heat and mass transfer within that system.

The overall objective of this investigation is to quantify and examine the flame behavior of benzoic resin over the surface induction plate as a function of surface temperature using liquefied petroleum gas ignitor. There is no report for biomass flame characteristics analysis as a function of surface temperature till date. Henceforth, an induction heating plate has been deployed as a surface heating source and LPG flame ignitor as an external ignition source for acquiring the entire flame structure of the benzoic resin solid fuel pellets under the regimes of varying heat distribution and time.

## 2. Methodology

Fig. 2 presents the gas chromatography (GC) curve of benzoic resin solid pellet. As it can be seen from the figure that there is a gradual and sporadic variation of peak for increasing retention time. The RT (retention) values show the main chemical components of the benzoic resin. The corresponding Table 1 presents the parameters obtained from the benzoic resin chromatogram and the chemical components. The benzoic resin was dissolved in toluene and was injected in the GC for the analysis. Afterwards, FESEM and EDAX methods have been employed for microstructural characterization and chemical component identification. The results from EDAX analysis showed a chemical composition of 70% Carbon, 21% Oxygen, 3% Calcium, 4% Potassium, and 2% Chlorine (Fig. 3 h).

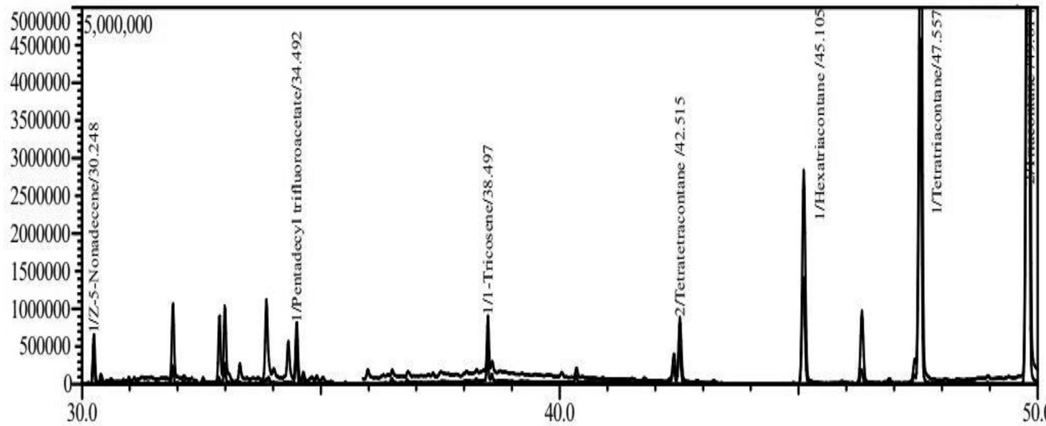


**Fig. 2.** Gas chromatogram of Benzoic Resin.

**Table 1**
Benzoic resin GC report.

| Peak | Retention Time (min) | Name | Area | Percentage of Area |
|---|---|---|---|---|
| 1 | 30.248 | Z-5-Nonadecene | 1756018 | 0.17 |
| 2 | 34.492 | Pentadecyl trifluoroacetate | 2143723 | 0.20 |
| 3 | 38.497 | 1-Tricosene | 1855599 | 0.18 |
| 4 | 42.515 | Tetratetracontane | 2673103 | 0.25 |
| 5 | 45.105 | Hexatriacontane | 11956664 | 1.13 |
| 6 | 47.557 | Tetratriacontane | 36257709 | 3.43 |
| 7 | 49.814 | Tricontane | 74912083 | 7.08 |
| 8 | 51.915 | Eicosane | 109207215 | 10.33 |
| 9 | 53.876 | Pentatriacontane | 143957170 | 13.61 |
| 10 | 55.712 | Tetrapentacontane | 150387238 | 14.22 |
| 11 | 57.449 | Hexacontane | 155284458 | 14.69 |
| 12 | 59.090 | Tetracosane | 123692087 | 11.69 |
| 13 | 60.665 | Octacosane | 107242618 | 10.14 |
| 14 | 62.230 | Tritetracontane | 67686665 | 6.40 |
| 15 | 64.022 | Hexatriacontane | 45207934 | 4.28 |
| 16 | 66.126 | Dotetracontane | 6503893 | 0.62 |
| 17 | 68.606 | Heneicosane | 16681936 | 1.58 |
| | | | 1057346113 | 100.0 |

Fig. 3a–g shows the field emission scanning electron (FESEM) microscopic images of the benzoic pellet. A total of seven images were obtained for the analysis under the magnifications of 2 μm, 20 μm, 100 μm, and 200 nm. Honeycomb structures were observed in Fig. 3 d) and g) under 20 μm and 200 nm magnification ranges, indicated in orange squares. Moreover, yellow squares in Fig. 3) a), b), c), e) and f) indicate the binder. Enlarged view of each FESEM image can be seen in the supplementary file. Table 2 shows the major fuel properties of benzoic resin and it has been compared with other coal grades.

The schematic layout of the experimental setup is given in Fig. 4. It consists of an induction heater covered with a steel plate. Over this, the benzoic resin solid fuel is placed for flame test. The induction heater is connected to AC source and it is equipped with time and temperature display. Induction heating is gradually becoming popular for ignition, flame and combustion analysis of both solid and liquid fuels. The liquefied petroleum gas flame ignitor was placed aside to trigger the ignition on benzoic solid and on the other side, a closed circuit television (CCTV) camera is placed to capture the flame images. The CCTV camera is connected to CCTV unit and then to a data acquisition system (DAS). But, induction heater is directly connected to data acquisition system unit and then overall connected to computer system, which is installed with AVL-415 6000 Delta version software package to analyze the combustion and heat release rates of a fuel over induction heating plate.

## 3. Results and discussions

### 3.1. Flame characteristics

This section critically discusses about the changing flame characteristics of the benzoic resin as a function of surface temperature. At the beginning of the experiment, there is neither spark nor ignition, but there is an enormous amount of smoke release. The objective of this work is to acquire varying images of benzoic resin flames for which camphor nanoparticles were sprayed on the top circular face of the benzoic solid and a new solid is placed for each test. Analyzing the characteristics of camphor nanoparticles is beyond the core theme of this paper. Nevertheless, the camphor nanoparticles on the top face of benzoic solid pellet act only as a catalyst to accelerate the exothermic reaction and also acting as a heat transfer agent for transferring heat to the middle and bottom zones of the benzoic resin. Actually, this experiment was conducted to acquire the varying flames and subsequent capture of its images. Besides, these nanoparticles do not change or modify the heating rate and volatility of benzoic resin [4]. Furthermore, camphor nanoparticles would catch fire upon flame impulse and increase the

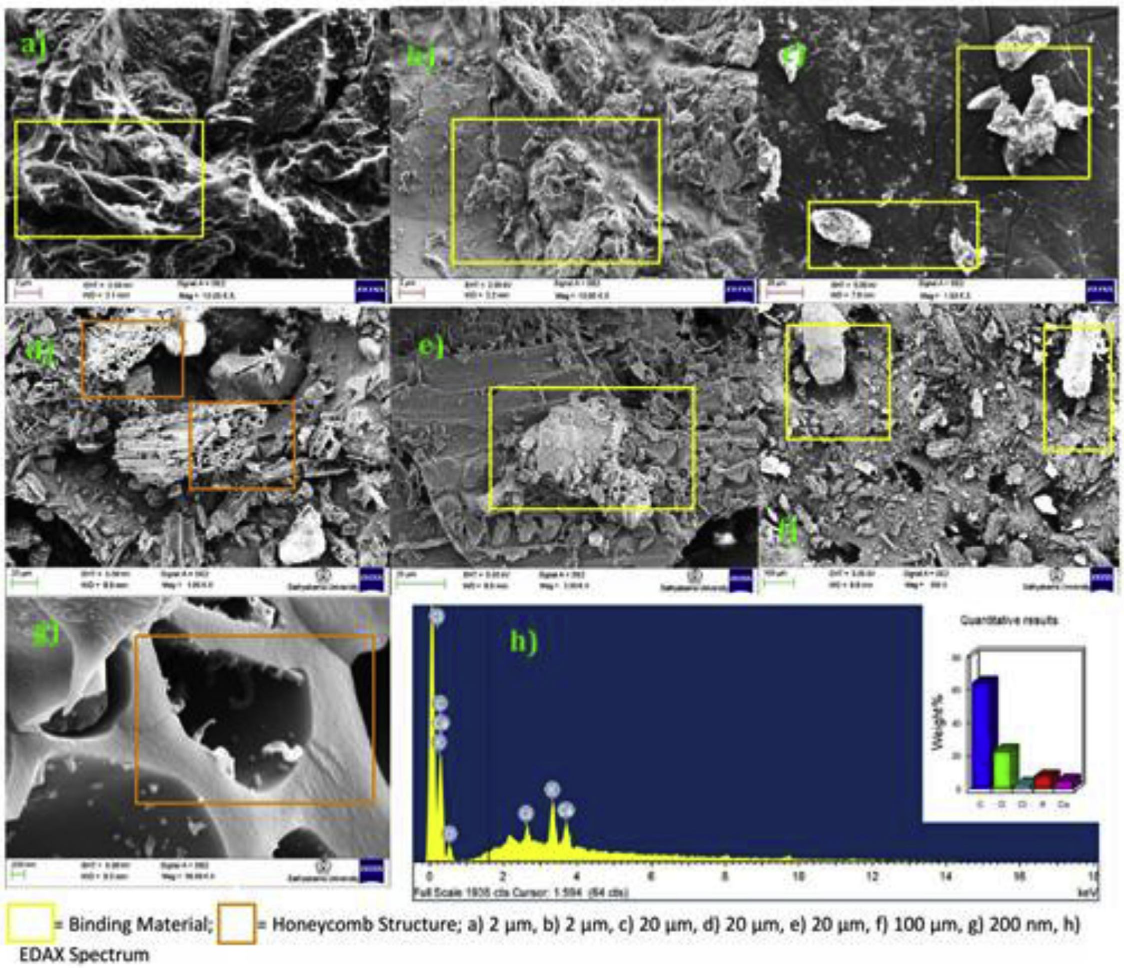


**Fig. 3.** Fesem images and EDAX Spectrum of benzoic resin.

**Table 2**
Major fuel properties of benzoic resin and other coals [4].

| Properties | Unit | Lignite | Bituminous | Anthracite | Benzoic Resin |
|---|---|---|---|---|---|
| Gross Calorific Value | (kJ/kg) | 16,410.57 | 23,326.00 | 33,445.71 | 26,004.92 |
| Ignition Temperature | (°C) | 273 | 440 | 730 | 70 |
| Volatile Initial Release Temperature | (°C) | 150 | 242 | 395 | 90 |
| Electrical Conductivity | µS/cm | 876 | 1293 | 2944 | 1620 |
| Bulk Density | (kg/m$^3$) | 645 | 728 | 890 | 334 |
| Ash Content | Wt (%) | 4.3 | 8.1 | 14.5 | 19.2 |
| Carbon Content | Wt %) | 32.3 | 53.8 | 82.4 | 72.6 |
| Moisture Content | Wt %) | 38 | 7.9 | 13.8 | 2.6 |
| Sulphur Content | Wt %) | 0.41 | 0.74 | 0.66 | 0 |

combustion rate. Figs. 5–7 show the various flame behavior of benzoic resin solid over the induction heating plate with surface temperatures of 70 °C, 110 °C, 130 °C, 160 °C, 180 °C, 210 °C, 240 °C, and 270 °C. Initially, during the beginning of the experiment, the benzoic resin solid fuel underwent physical ignition delay. It is a process in which the benzoic solid vaporizes and will mix with air and this ignition delay reduced at higher surface temperatures. Essentially, ignition delay is characterized by the time interval between the start of liquefied petroleum gas flame (LPG) impulse and start of benzoic resin ignition. Actually, it is described by the long time taken for the benzoic resin solid pellet embedded with camphor nanoparticles to ignite even after applying the LPG flame. Certainly, air plays a major role in affecting the ignition and the flame behavior of benzoic resin over a surface induction heater. In this scenario, the ignition delay is mainly dominated by the physical delay that is differences in the air-fuel mass balance, surrounding temperature, vaporization (volatility), etc.

It can be seen from Fig. 5 (a) that benzoic resin exhibits both turbulent and transition flames upon ignition at the surface temperature of 70 °C. In the fuel property table it is clear that the ignition temperature of benzoic resin is near 70 °C, hence, it indicates that the ignition and flame can neither be detected nor partially achieved with a minimum surface temperature, which is confirmed by this experiment. The same occurrence was noted

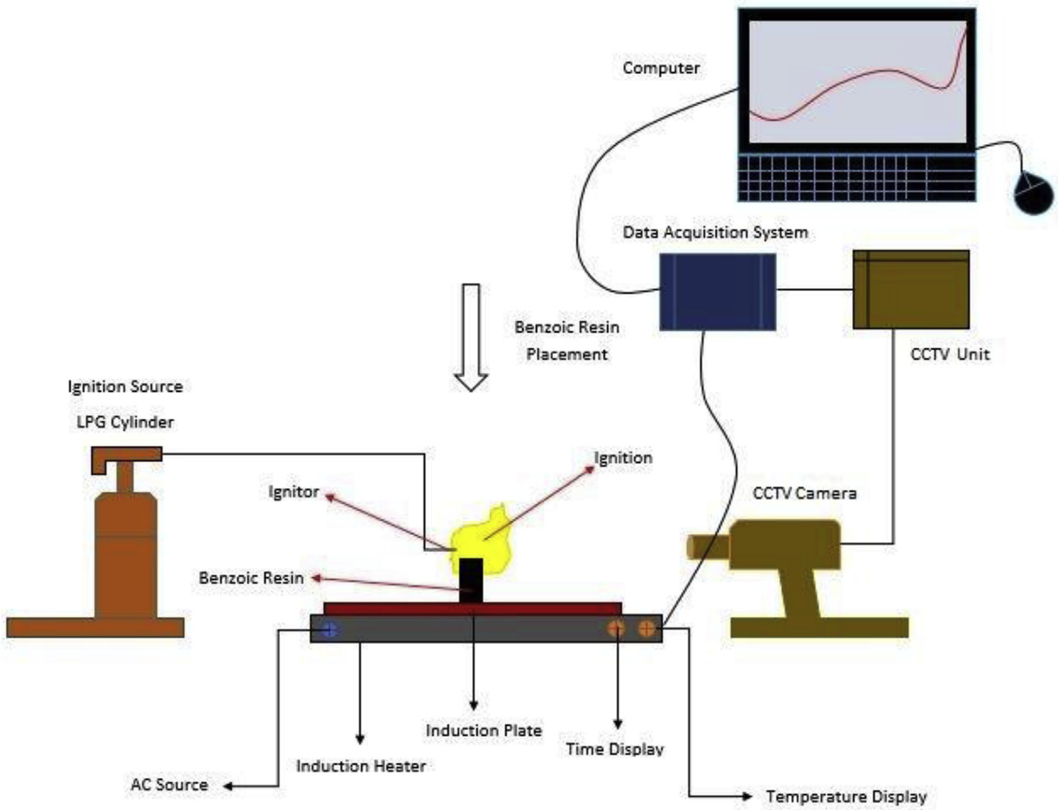


**Fig. 4.** Schematic diagram of experimental setup.

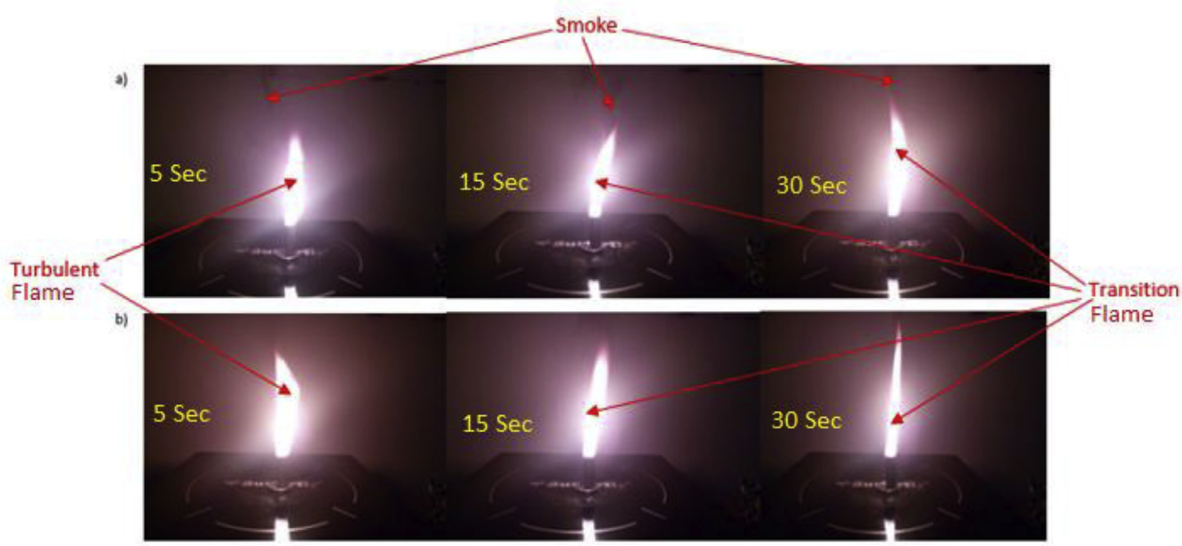


**Fig. 5.** Benzoic Resin Exhibiting Varying Flames Over Ignition: a) 70 °C surface temperature, b) 110 °C Surface Temperature.

even at 110 °C surface temperature, but only difference is the flame length. At this surface temperature, the transition flame length is quite higher than that of the previous surface temperature. It can be observed in this set of experiments that there is a release of smoke during and after ignition in a laminar and transition movement. Also, it can be implied that there is a large exchange of heat energy between the bottom circular face of benzoic resin and induction surface plate. Since the heat is transferred from induction plate to benzoic resin through conduction mechanism and then, upon ignition a radiative heat is liberated to the surroundings. This shows that the benzoic resin has a high amount of enthalpy and has high capacity of producing any mechanical work. It can be stated that at these two surface temperatures the benzoic resin over induction plate display a slight unstable flame. Generally, the stability of solid

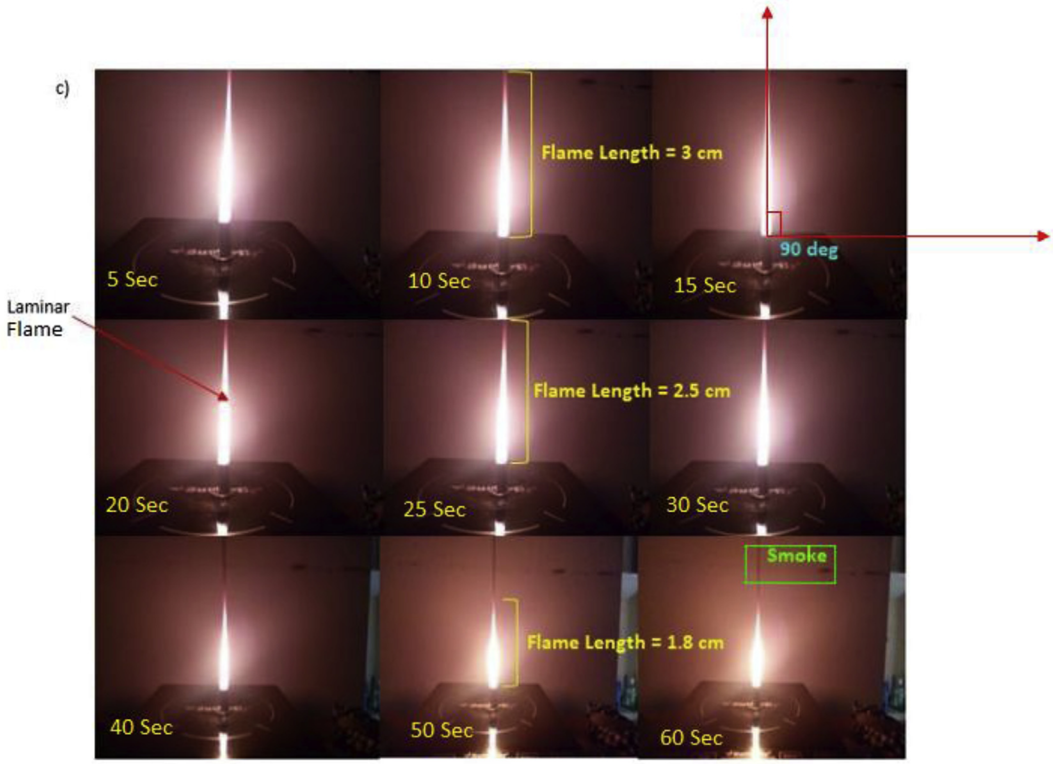


**Fig. 6.** Benzoic resin exhibiting a laminar flame at 160 °C surface temperature.

fuel flames can be characterized by the ignition stability and flame propagation [12]. In this case, with the help of charged couple device (CCD) camera and visible inspection, the flames oscillation frequency with respect to surface temperature increase has been measured and this turbulent and transition flames guides one to quantify the flame stability of benzoic resin solid fuel. In this scenario, the flame stability was characterized by lift-off height and there was no observation nor evidence for lift-off. Since, bottom zone of the flame (inner core area) is absolutely wetting on the benzoic solid resin top circular face. Also, it can be implied that the room temperature and surrounding air ratio may affect the flame stability and propagation as well.

Interestingly, a laminar flame (with 90° angle) was observed at the surface temperature of 160 °C as shown in Fig. 6. It can be implicated that the nature of these flames may be due to uniform surface temperature. During heating of induction plate, the heat flux will be randomly distributed across all the sides of the plate and as a result, turbulence and transition were observed at 70 °C and 110 °C respectively. After some time, the heat flux over an induction plate will be evenly distributed, which means a uniform or steady state heat flux will prevail in the entire area of the surface plate and subsequently, the benzoic resin will show a laminar flame. A heterogeneous condition was occurring in this case, in which the characterization was evaluated by the exchange of heat and induction plate with the bottom circular face of the benzoic solid [14]. It can be noted from Fig. 6 that the flame length (distance between the flame bottom and tip) of the top three images were 3 cm and the middle flame images accounts for 2.5 cm, and finally, bottom images are found to be 1.8 cm. Actually, there is a reduction in the flame length for increasing time and this is mainly due to the sublimation rate of the camphor nanoparticles. Moreover, the high presence of camphor nanoparticles over benzoic solid produces a higher flame length and after gradual increase in time and sublimation rate the flame length is decreased. Altogether, increasing time, sublimation rate and differences in lab temperature govern the flame length. Even, at 270 °C surface temperature, the flame temperature (and surrounding lab environment) gets reduced and as a result the flame length gradually shortens, as it is shown in Fig. 7. Here the degree of ignition and flame nature are same, but the difference is only in the flame length. In fact, the length and the propagation of flame is a function of its temperature regardless of surface and any thermal system inlet conditions [15,16], and [17]. Furthermore, at the initial level, camphor nanoparticles over the top face of the basic resin produces flame and heat transfer to the middle and bottom zones of the benzoic solid pellet. As time exceeds the amount of camphor nanoparticles gets reduced that is sublime and subsequently, flame length is gradually reduced. The flame gets worn out after complete burning of camphor nanoparticles. Initially, the flame is observed from the resin and after that it dies out. It should be remembered that the flame length reduction does not alter nor affects the heat release rate of the benzoic resin. Typically, upon heating of benzoic solid produces a tremendous amount of smoke and fumes. But, already, it was indicated that the main goal of adding camphor nanoparticles over the top face of benzoic solid is only to capture the flame image.

### 3.2. Mathematical model

This section presents a mathematical model for the evaluation and prediction of ignition, heat release rate and changing flame structures (including length) of the benzoic resin solid fuel under the surface induction heating regime.

$$\alpha_i = \frac{\Delta\psi}{\pi(r^2 + 6)} \tag{1}$$

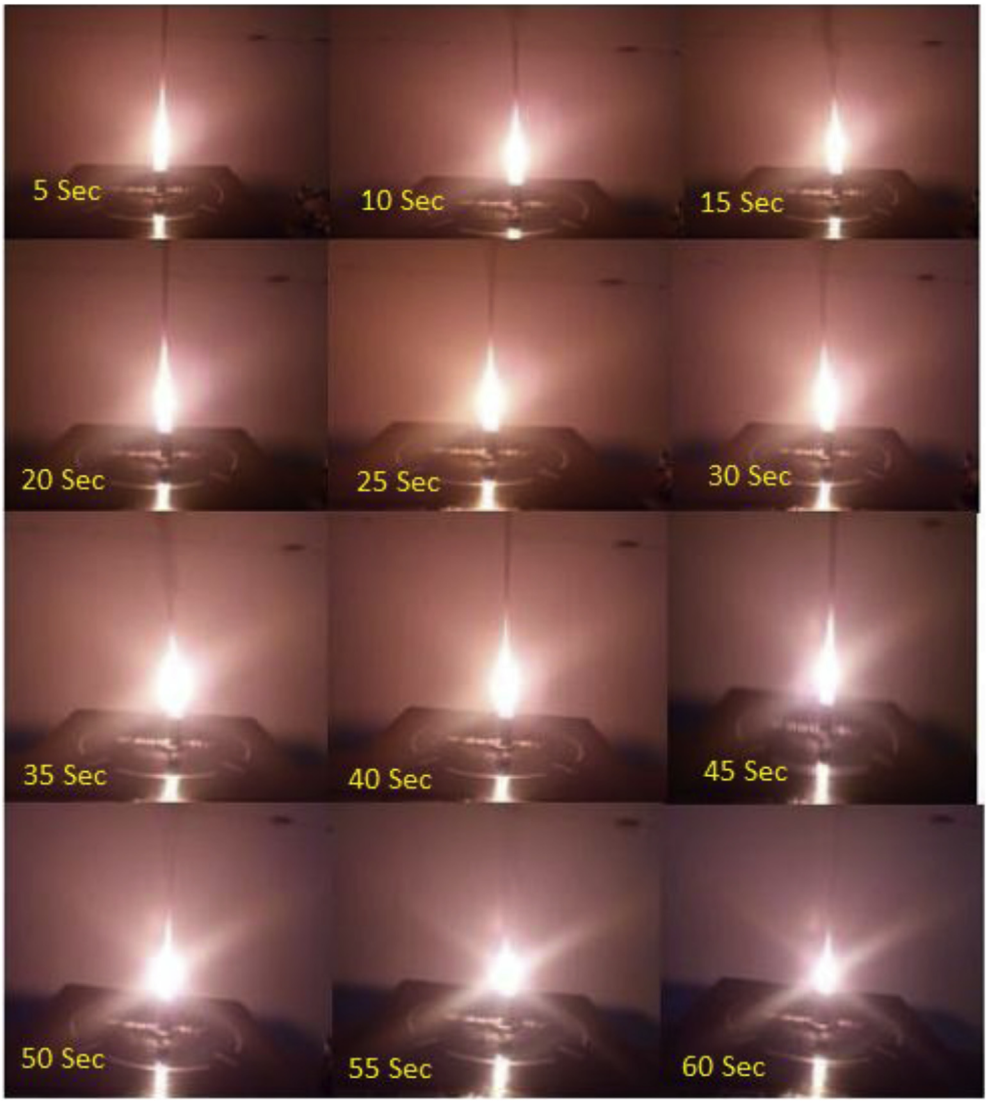


**Fig. 7.** Benzoic resin exhibiting a laminar short length flame at 270 °C surface temperature.

The overall heat liberation after ignition from the benzoic resin is given by:

$$Q_{chr} = \frac{t\frac{dQ}{dt}\left(-Q_s - Q_{if}\right)}{(T_{max} - T_{min})\Delta H\left(\frac{1}{\beta_{t_2}} - \frac{1}{\beta_{t_1}}\right)} \tag{2}$$

This equation can be used for calculating the heat release rate over a surface plate operating through induction heating. The flame propagation in the z-direction [18] is given by the following equation:

$$\rho u_z r\frac{\partial u_z}{\partial z} + \rho u_r r\frac{\partial u_z}{\partial_r} = -r\frac{\partial p}{\partial z} + \frac{\partial}{\partial r}\left(\mu r\frac{\partial u_z}{\partial r}\right) \tag{3}$$

Flame propagation in polar coordinate is as follows:

$$\frac{\partial^2 u}{\partial r^2} + \frac{1}{r}\frac{\partial u}{\partial r} + \frac{1}{r^2}\frac{\partial^2 u}{\partial \theta^2} = \frac{1}{\alpha^2}\frac{\partial u}{\partial t} \tag{4}$$

Thus, equation (3) can be modified as below:

$$\theta T_{\alpha f}\left(u_z r\frac{\partial u_z}{\partial z} + \rho u_r r\frac{\partial u_z}{\partial_r}\right) = -\theta T_{-\alpha f}\left(r\frac{\partial p}{\partial z} + \frac{\partial}{\partial r}\left(\mu r\frac{\partial u_z}{\partial r}\right)\right) \tag{5}$$

Uniform heat flux over the induction plate is given by:

$$K_{c\phi_c} = \left(\frac{T_{max} - T_{min}}{\Delta H}\right)2\pi r(h+r) \tag{6}$$

Varying heat flux over induction plate is given by:

$$K_{c\phi_v} = \Delta H.\ 2\pi r(h+r)\left(\frac{T_{max} - T_{min}}{L}\right) \tag{7}$$

The general equation for flame length with respect to angle is given as follows:

$$F_L = \theta u\alpha[T_{bz} - T_{tz}] \tag{8}$$

Substituting equation (1) in (8), we have:

$$F_L = \frac{\theta u\Delta\psi[T_{bz} - T_{tz}]}{\pi(r^2+6)} \tag{9}$$

Then, the enthalpy and the sublimation rate of benzoic resin is given by:

$$\Delta H = U + PV \tag{10}$$

$$\zeta = \frac{m_i - m_{\Delta t}}{m_i - m_\beta} \tag{11}$$

Where.

$m_{\Delta t}$ is the sample mass that varies with time, $m_i$ is the initial mass of the sample and $m_\beta$ is the remaining sample mass after ignition.

Let us present an analytical model with respect to surface temperature.

$$\Delta\lambda = \frac{\text{Temperature difference between bottom and top zones of benzoic resin}}{\text{Change in heat flux over the induction plate}}$$

Therefore,

$$\Delta\lambda = \left(\frac{(u_1^2 - u_2^2)}{2T_s} + \frac{T_{bz} - T_{tz}}{2T_s}\right) \Bigg/ \left[\left(\frac{t_1^2 - t_2^2}{2T_s}\right) + \left(\frac{u_1^2 - u_2^2}{2T_s}\right) + \left(\frac{T_{bz}^2 - T_{tz}^2}{2T_s}\right)\right] \tag{12}$$

$$\Delta\lambda = \frac{\left(u_1^2 - u_2^2\right) + \left(T_{bz}^2 - T_{tz}^2\right)}{\left(t_1^2 - t_2^2\right) + \left(u_1^2 - u_2^2\right) + \left(T_{bz}^2 - T_{tz}^2\right)}$$

$$\Delta\lambda = \frac{\left(t_1^2 - t_2^2\right) + \left(u_1^2 - u_2^2\right) + \left(T_{bz}^2 - T_{tz}^2\right) - \left(t_1^2 - t_2^2\right)}{\left(t_1^2 - t_2^2\right) + \left(u_1^2 - u_2^2\right) + \left(T_{bz}^2 - T_{tz}^2\right)} \tag{13}$$

$$= 1 - \frac{\left(t_1^2 - t_2^2\right)}{\left(t_1^2 - t_2^2\right) + \left(u_1^2 - u_2^2\right) + \left(T_{bz}^2 - T_{tz}^2\right)}$$

The change in pressure energy of the flame can be mentioned as:

$$\Delta P_e = \frac{t_1^2 - t_2^2}{2T_s} + \frac{u_1^2 - u_2^2}{2T_s} + \frac{T_{bz}^2 - T_{tz}^2}{2T_s} \tag{14}$$

$$2T_s\Delta P_e = \left(t_1^2 - t_2^2\right) + \left(u_1^2 - u_2^2\right) + \left(T_{bz}^2 - T_{tz}^2\right) \tag{15}$$

Equation (13) can be further written as:

$$\Delta\lambda = 1 - \frac{(t_1^2 - t_2^2)}{2T_s\Delta P_e} \tag{16}$$

With the addition of flame length term to equation (16), we get:

$$\Delta\lambda = 1 - \frac{(t_1^2 - t_2^2)}{2T_s\Delta P_e} + \theta F_L \tag{17}$$

By substituting equation (9) in the above equation, we get:

$$\Delta\lambda = 1 - \frac{(t_1^2 - t_2^2)}{2T_s\Delta P_e} + \theta\left[\frac{\theta u\Delta\psi[T_{bz} - T_{tz}]}{\pi(r^2 + 6)}\right] = 1 - \frac{(t_1^2 - t_2^2)}{2T_s\Delta P_e} + \theta^2\frac{u\Delta\psi[\theta T_{bz} - \theta T_{tz}]}{\pi(r^2 + 6)} \tag{18}$$

Finally,

$$\Delta\lambda = 1 - \frac{(t_1^2 - t_2^2)}{2T_s\Delta P_e} + \theta\left[\frac{u\Delta\psi\theta[T_{bz} - T_{tz}]}{\pi(r^2 + 6)}\right] \tag{19}$$

Therefore, the above equation that is required analytical solution, accounts for benzoic resin flame stability with respect to surface temperature. Lastly, based on the experimentation, we present a mathematical condition ($\gamma_f$) for different flame characteristics of benzoic resin solid fuel with respect to induction heating surface temperature.

$$\gamma_f = \begin{cases} \Delta\lambda \geq T_s, & \textit{Laminar Flame} \\ \Delta\lambda \leq T_s, & \textit{Transition Flame} \\ \Delta\lambda < T_s, & \textit{Turbulent Flame} \end{cases} \tag{20}$$

Therefore, a mathematical model for changing flame behaviors of benzoic solid fuel was successfully performed as a function of surface temperature.

### 3.3. Heat release rate analysis

This section discusses and analyze the heat release rate (HRR) characteristics of benzoic resin. These heat release curves were acquired by the AVL combustion analyzer software during combustion and flame tests. Figs. 8 and 9 present the benzoic resin HRR curves for increasing induction heating surface temperatures and combustion time. As it can be viewed from Fig. 8 that the rate of heat release from benzoic resin over the induction thermal plate is gradually increasing. Initially, at 70 °C surface temperature 90 J/s was recorded and then 128 J/s heat release was noted at the plate surface temperature of 100 °C. Between these two surface temperatures, there is a rise of 38 J/s of heat release. Then, at 130 °C, the heat release rate (HRR) value is found to be 152 J/s and a breakthrough of heat release rate is observed at 180 °C surface temperature, which gives the value of 196 J/s. Generally, the heat release rate is linked to the gross calorific value (GVC) of the fuel and this benzoic solid resin exhibit good calorific content, which is higher than low to medium rank coals. Finally, the HRR curve is soaring to 280 J/s at the surface temperature of 270 °C, which is considered as the maximum value.

The maximum heat release rate corresponding to each combustion time is shown in Fig. 9. Even in this case, 95 J/s was initially observed after the combustion time of 60s. Then, 140 J/s was noted for 180 s and soaring to a maximum of 316 J/s. This value is obtained for the combustion time of 900 s and leaving a large quantity of ash as a residue. Even this phenomenon of ash production was reported in the literature [4] during an ignition test of the benzoic resin over induction heating plate. In this case also, it is stated that the solid

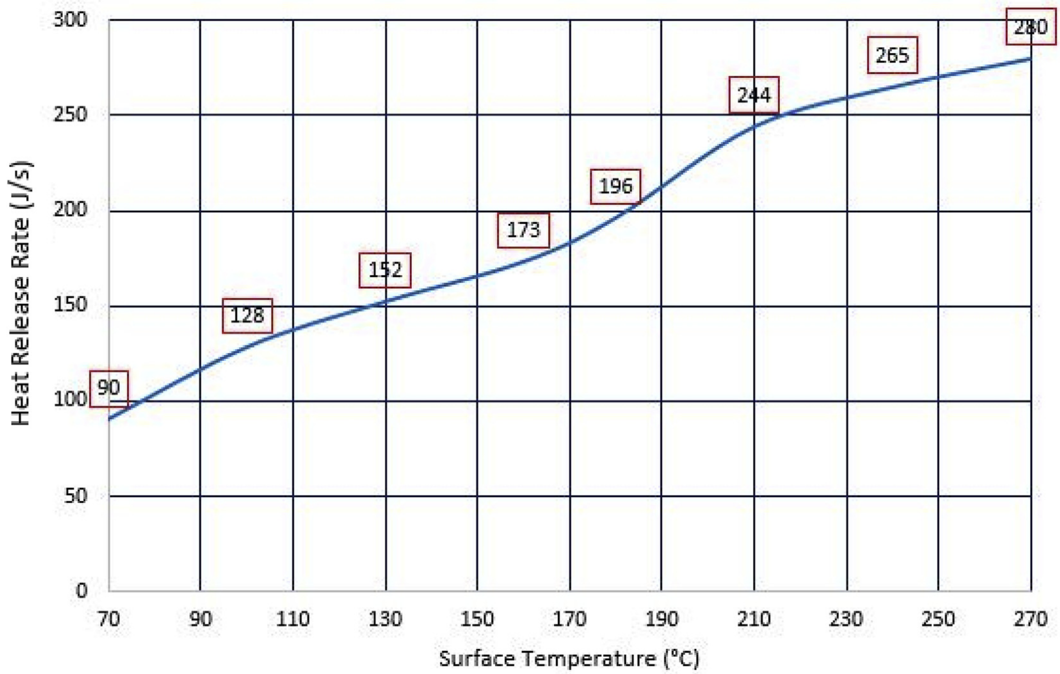


**Fig. 8.** Heat release rate for varying surface temperature.

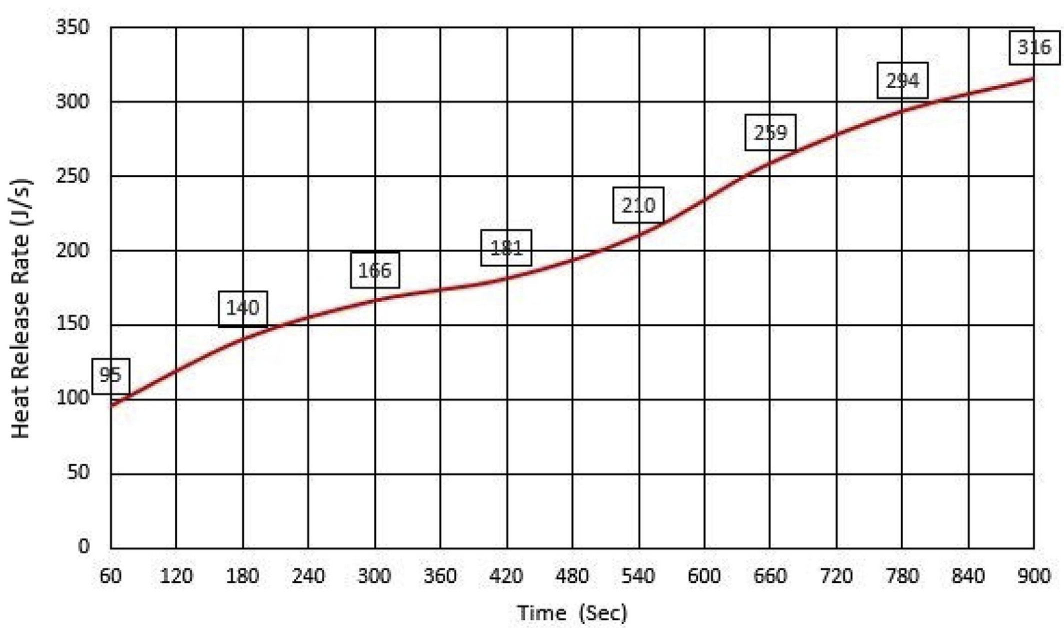


**Fig. 9.** Heat release rate for varying time.

fuel benzoic resin ignites rapidly and produces a massive heat release rate with complement smoke in tandem (smoke followed by flame). The higher heat release rate was observed for the combustion time of 15 min, which indicates that the energy content per unit mass is higher compared with lignite and bituminous coals. Therefore, this illustrates the benzoic solid fuel at the higher burning rate is attributed to the enhancement of diffusion burning phase on account of its oxygen content. Unlike liquid and gaseous fuels, the GCV of solid fuels is comparatively low, and consequently, these fuels require tremendous energy to accelerate the combustion and heat release rates [19]. Additionally, it should be observed that Figs. 8 and 9 exhibits similar curves and this is due to the fact that surface temperature and time are directly proportional.

It can be seen from Fig. 10a) and b) that there is a close correlation between experimental, analytical and statistical models. The correlation was obtained by plotting surface temperature (°C) vs heat release rate (J/s) and another being surface temperature (°C) vs flame transition time (s). A multiple linear regression model in SPSS (Statical Package for Social Science), a statistical simulation tool was

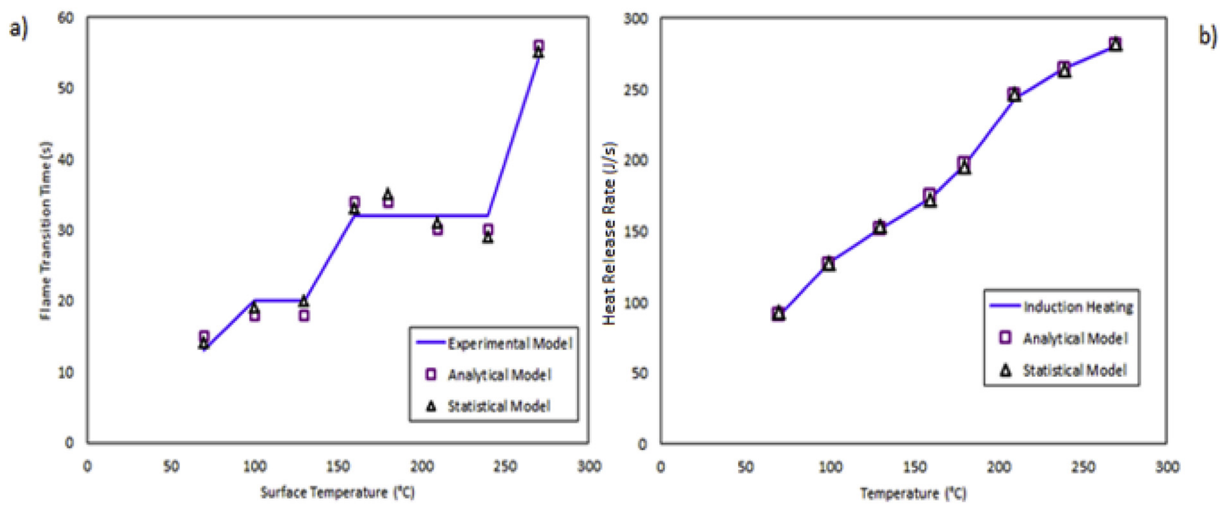


**Fig. 10.** Model validation.

employed to find the accuracy and reliability of the experimental model. On the whole, the model revealed good agreement and there were no major differences in the model accuracy. Therefore, it can be stated that this model is reliable for laboratory and industry based analysis of flame and combustion characteristics of the benzoic resin solid fuel.

Thus, this paper has successfully highlighted the importance of the benzoic resin solid fuel flame characteristics as a function of surface temperature and these experimental outcomes suggest that the benzoic resin could be a potential supplement to coal and charcoal in the foreseeable future.

## 4. Conclusions

This paper successfully demonstrated the changing flame characteristics of benzoic resin pellets as a function of surface temperature and time. Based on the experimental results following conclusions can be drawn:

a) At 70 °C surface temperature, the benzoic resin exhibits both turbulent and transition flames. The flames are accompanied by a linear release of smoke in the upward direction. The flames stabilize to laminar condition at the surface temperature of 160 °C, which has the flame length of 3 cm, 2.5 cm, and 1.8 cm with respect to time.
b) Even at 270 °C the benzoic resin exposed a laminar flame with very short lengths due to drop in the flame temperature. Additionally, an analytical model was successfully developed and executed for the evaluation and prediction of the varying flame behavior of benzoic resin.
c) A linear increase in heat release rate was observed for varying surface temperatures and combustion time. The maximum heat release rate of 280 J/s was achieved at 270 °C surface temperatures and 316 J/s was achieved at the combustion time 900s. Furthermore, the experimental models were validated against the analytical and statistical models, which indicated good agreement.

## Acknowledgement

This research work was funded by Dawn Calorific Exports (Grant No: DCE-RF-002), Chennai, India and grateful to Mr. R. Kesavakumar, COO of this company for technical and financial supports. Also, the corresponding author would like to thank Dr. Krishnaraj, Apex Biotech Training and Research Institute, Chennai for the acquisition on GC curve. Furthermore, Dr. B. Kanimozhi, Professor of Thermal Engineering at SIST-Chennai, India is thanked for FESEM acquisition and especial thanks to Dr. S. Senthil, Professor of Mechanical Engineering at KCET-Virudhunagar, TN, India for the help on the experimental setup. Most importantly, all authors heartily thank the anonymous reviewers for their constructive criticism and suggestions, which improved the overall quality of this paper.

## Appendix A. Supplementary data

Supplementary data to this article can be found online at https://doi.org/10.1016/j.renene.2019.09.061.

## Nomenclature

| | |
|---|---|
| $CO_2$ | *Carbon Dioxide* |
| *GC* | *Gas Chromatography* |
| *RT* | *Retention Time* |
| *MS* | *Mass Spectroscopy* |
| *LPG* | *Liquified Petroleum Gas* |
| *HRR* | *Heat Release Rate* |
| *GCV* | *Gross Calorific Value* |
| *CCD* | *Charged Coupled Device* |
| *PAD* | *Photodiode Array Detector* |
| *DAS* | *Data Acqusition System* |
| *CCTV* | *Closed Circuit Television* |
| *EDAX* | *Energy Dispersive X–Ray Analysis* |
| *SPSS* | *Statistical Package for Social Science* |
| *HPLC* | *High Performance Liquid Chromatography* |
| *FESEM* | *Field Emission Scanning Electron Microscope* |
| $r$ | *Radius (cm)* |
| $t$ | *Time (s)* |
| $z$ | *z coordinate* |
| $u$ | *Internal energy (J/kg)* |
| $L$ | *Length (cm)* |
| $h$ | *Height (cm)* |
| $P$ | *Pressure (bar)* |
| $V$ | *Volume* ($m^3$) |
| $m$ | *Mass (kg)* |
| $t_1$ | *Initial time (s)* |
| $t_2$ | *Final time (s)* |

| | |
|---|---|
| $u_1$ | *Initial internal energy* $(J/kg)$ |
| $u_2$ | *Final internal energy* $(J/kg)$ |
| $m_i$ | *Initial mass* $(kg)$ |
| $m_{\Delta t}$ | *Change of mass with respect to changing time* $(kg)$ |
| $m_\beta$ | *Remaining mass* $(kg)$ |
| $Q_s$ | *Heat content over solid fuel* $(J/A)$ |
| $Q_{if}$ | *Heat content between the plate and bottom zone of benzoic resin interface* $(JA)$ |
| $Q_{chr}$ | *Cumulative Heat Liberation* (J/S) |
| $T_{\max}$ | *Maximum temperature* $(^\circ C)$ |
| $T_{\min}$ | *Minimum temperature* $(^\circ C)$ |
| $T_s$ | *Surface temperature* $(^\circ C)$ |
| $T_{bz}$ | *Temperature of bottom zone of benzoic resin* $(^\circ C)$ |
| $T_{tz}$ | *Temperature of top zone of benzoic resin* $(^\circ C)$ |
| $T_{\alpha f}$ | *Temperature of flame propagation* $(^\circ C)$ |
| $K_{c\phi c}$ | *Uniform heat flux over induction plate* $(W\,m^{-2})$ |
| $K_{c\phi v}$ | *Varying heat flux over induction plate* $(W\,m^{-2})$ |
| $F_L$ | *Flame length* $(cm)$ |
| $\theta$ | *Angle* (*degree*) |
| $\alpha_i$ | *Ignition impact with respect to the ith time* (*initial time*) |
| $\rho$ | *Density* $(kg/m^3)$ |
| $\mu$ | *gas viscosity* $(cP)$ |
| $\psi$ | *Thermal potential* $(J/K)$ |
| $\alpha$ | *Heat flow* $(J/s)$ |
| $\beta$ | *Energy conversion efficiency* (%) |
| $\zeta$ | *Sublimation rate* $(J/kg)$ |
| $\gamma_f$ | *Mathematical condition of flame nature over surface induction heater* |
| $\Delta H$ | *Change in enthalpy* $(J/kg)$ |
| $\Delta P_e$ | *Change in pressure energy* $(^\circ C)$ |
| $\Delta\psi$ | *Change in thermal potential* $(J/K)$ |
| $\Delta\lambda$ | $\frac{\text{Temperature difference between bottom and top zones of benzoic resin}}{\text{Change in heat flux over the induction plate}}$ |

## References


[1] N. Bilandzija, N. Voca, B. Jelcic, V. Jurisic, A. Matin, M. Grubor, T. Kricka, Evaluation of Croatian agricultural biomass energy potential, Renew. Sustain. Energy Rev. 93 (2018) 225–230.

[2] M.,R. Karim, J. Naser, Numerical modelling of solid biomass combustion: difficulties in initiating the fixed bed combustion, Energy Procedia 110 (2017) 390–395.

[3] B. Lin, M. Xu, Regional differences on $CO_2$ emission efficiency in metallurgical industry of China, Energy Policy 120 (2018) 302–311.

[4] V. Pranesh, S. Balasubramanian, S. Mahalingam, S. Ravikumar, T.,C. Michael, B. Kanimozhi, Ignition behavior of benzoic resin solid fuel pellets over a surface induction heating plate using a liquefied petroleum gas flame ignitor, Energy Fuels 32 (2018) 7888–7897.

[5] S. Cunningham, Cunningham's Encyclopedia of Magical Herbs, first ed., Llewellyn Publications, Woodbury, MN, 2017.

[6] P. Burger, A. Casale, A. Kerdudo, T. Michel, R. Laville, F. Chagnaud, X. Fernandez, New insights in the chemical composition of benzoin balsams, Food Chem. 210 (2016) 613–622.

[7] G. Hyams, Incense: Rituals, Mystery, Lore, first ed., Chronicle Books, San Francisco, CA, 2003.

[8] M. Kashio, D. Johnson, *Monograph On Benzoin*. Balsamic Resin from Styrax Species, Food and Agriculture Organization of the United Nations Regional Office for Asia and the Pacific, Bangkok, Thailand, 2001, pp. 7–47.

[9] M. Hovaneissian, P. Archier, C. Mathe, G. Culioli, C. Vieillescazes, Analytical investigation of styrax and benzoin balsams by HPLC-PAD-fluorimetry and GC-MS, Phytochem. Anal. 19 (2008) 301–310.

[10] X. Fernandez, C. Castel, L. Lizzani-Cuvelier, C. Delbecque, S.,P. Venzal, Volatile constituents of benzoin gums: Siam and Sumatra, part 3. Fast characterization with an electronic nose, Flavour Fragrance J. 21 (2006) 439–446.

[11] C. Katzer, K. Babul, M. Klatt, H.J. Krautz, Quantitative and qualitative relationship between swirl burner operating conditions and pulverized coal flame length, Fuel Process. Technol. 156 (2017) 138–155.

[12] J. Smart, G. Lu, Y. Yan, G. Riley, Characterisation of an oxy-coal flame through digital imaging, Combust. Flame 157 (2010) 1132–1139.

[13] Y. Bai, K. Luo, K. Qiu, J. Fan, Numerical investigation of two-phase flame structures in a simplified coal jet flame, Fuel 182 (2016) 944–957.

[14] S. Carra, Homogeneous and Heterogeneous Combustion. Combustion and Detonation. Milano, Italy: Encyclopedia of Hydrocarbons, 2017, pp. 413–416.

[15] C.E. Baukal, B. Gebhart, Surface condition effects on flame impingement heat transfer, Exp. Therm. Fluid Sci. 15 (1997) 323–335.

[16] X.Y. Zhao, D.C. Haworth, Transported PDF modeling of pulverized coal jet flames, Combust. Flame 161 (2014) 1866–1882.

[17] B. Wu, S.P. Roy, X. Zhao, M.F. Modest, Effect of multiphase radiation on coal combustion in a pulverized coal jet flame, J. Quant. Spectrosc. Radiat. Transf. 197 (2017) 154–165.

[18] I.,H. Pitsch, Turbulent Non-premixed Combustion, RTWH Aachen University, Germany, 2014.

[19] A.S. Mideen, Engineering Chemistry-II, first ed., Airwalk Publications, 2015, pp. 27–45. ISBN; 978-9384893354.